

Response to anonymous referee #1

Lorena Moreira

August 27, 2015

Firstly, we thank the Anonymous Referee #1 for the useful and valuable comments, which provided insights that helped significantly to improve the paper. Secondly, we would like to stress that this publication really provides new findings, since the trend study of the GROMOS dataset has not been independently published yet. Steinbrecht *et al.* (2006) has used the GROMOS data mixed with the lidar data at Hohenpeissenberg to calculate the ozone trends from 1997 to 2005. In the WMO (2014) the GROMOS data (1994 to 2012) is used together with the Payerne station data, as far we can understand from Chapter 2 of WMO (2014). In addition, the trend profile of the microwave instruments is hidden by other lines in Figure 2-11 of WMO (2014). The important overview on trends in WMO (2014) cannot be a substitute for detailed trend studies of station data. Our study presents an harmonisation of the GROMOS dataset along with a trend estimation of the stratospheric ozone profiles from 1997 to 2015, calculated through a new robust method of trend estimation (von Clarmann *et al.*, 2010). We have revised the manuscript by following each one of your suggestions. This document includes all of your reported issues, as well as our responses in how we have addressed them.

General comments

1. **Comments from the referee:** There is no mention, where the data/homogenized time series from the GROMOS spectrometer are available. These data are probably available through the Network for the Detection of Atmospheric Composition, so this should be mentioned. Also it should be made clear which version of the data-set is available there - preferably the newest and most homogeneous version.

Author's response:

The harmonised GROMOS data since 1994 are available through the Network for the Detection of Atmospheric Composition Change (NDACC) on the NDACC public website at:

<http://ftp.cpc.ncep.noaa.gov/ndacc/station/bern/hdf/mwave/>

Author's changes in the manuscript:

Page 2, line 56
The ozone radiometer GROMOS is part of the NDACC-, hence our more than 20 years harmonised time series are available via <http://ftp.cpc.ncep.noaa.gov/ndacc/station/bern/hd>

2. **Comments from the referee:** Why is there no time series comparison with the NDACC lidar data from nearby stations at Hohenpeissenberg and Haute Provence? There

is also no comparison with any satellite records, although many satellite ozone records are available, e.g. during the 2009 to 2011 period when the two backend spectrometers were run in parallel.

Author’s response:

In Studer *et al.* (2013, ACPD) one can find a time series comparison with coinciding lidar measurements from the Observatoire Haute Provence (OHP), France, also with satellite measurements including MIPAS onboard ENVISAT, SABER onboard TIMED, MLS onboard EOS Aura and ACE-FTS onboard SCISAT-1; additionally, with ozonesondes launched from Payerne, Switzerland. The result being that the mean relative differences of GROMOS FTS and these independent instruments are less than 10% between 50 and 0.1 hPa.

Author’s changes in the manuscript: Page 3, line 58

Ozone time series from the GROMOS microwave radiometer were used for comparisons with lidar, ozonesondes and collocated satellite observations and for detection of long-term trends (Dumitru *et al.*, 2006; Steinbrecht *et al.*, 2006; Steinbrecht *et al.*, 2009; Keckhut *et al.*, 2010; van Gijssels *et al.*, 2010; Studer *et al.*, 2013; Delcloo and Kreher, 2013).

3. **Comments from the referee:** The multilinear fit residuals (middle panel in Fig. 6) are almost screaming for a parabolic trend in Eq. 1 (linear and quadratic terms in t). *Why has that not been tried? I think this should really be tested. It would be one “novel” aspect from the paper.*

Author’s response:

With all due respect to the referee, we felt that there are no physical reasons for a parabolic trend estimation of 17 years of stratospheric ozone profiles. Actually there is a polynomial of third degree in the residuals but a geophysical interpretation is questionable.

Author’s changes in the manuscript: No changes.

Specific comments

1. **Comments from the referee:** Pg. 16373, around line 20: I think the most important reference, Newchurch *et al.*, JGR, 2003 is missing here. Please add.

Author’s response:

No comments.

Author’s changes in the manuscript: Page 2, line 42

From the late 1990s, there were some measurements and model calculations indicating a turnaround in the decreasing ozone, suggesting that the negative ozone trends in the stratosphere would level out or even become positive (~~Huang *et al.*, 2014~~). Newchurch *et al.*, 2003

2. **Comments from the referee:** Pg. 16374, line 21: What is meant by harmonic variation? Probably the annual cycle and its harmonics (12 months, 6, 4, 3 and 24 months). Why not say so?

Author’s response:

No comments.

Author’s changes in the manuscript: Page 3, line 75

The regression model consists of an axis intercept, a linear trend, ~~harmonic variations~~ [sine waves](#), and several proxies.

3. **Comments from the referee:** Pg. 16376, line 11: “than” should be replaced by “as”

Author’s response:

No comments.

Author’s changes in the manuscript: Page 5, line 121

A sample of a calibrated ozone spectrum is given in Figure 2. It shows the ozone line recorded by the FFTS on the same winter morning ~~than~~ [as](#) the FB spectrum (Figure 1).

4. **Comments from the referee:** Pg. 16376, line 13: Is there a “spectrum” missing at the end?

Author’s response:

No comments.

Author’s changes in the manuscript: Page 5, line 123

The integration time is 30 minutes and no frequency binning is applied in the blue curve whereas the red line represents the 15 MHz frequency binned [spectrum](#).

5. **Comments from the referee:** Pg. 16377, line 13, 14: I do not understand the second part of that sentence? Why does the temperature at 2.5 km “exponentially approach” the surface temperature? Overall temperature at the surface and at 2.5 km will be highly correlated (except for diurnal cycle, or temperature inversion situations). This sentence should be reworded.

Author’s response:

T_{mean} depends on the temperature profile ($T(z)$) as well as on the absorption profile $\alpha(z, \nu)$ at a specific frequency. Since the number density is highest at low altitudes and the absorption is highest near the ground, T_{mean} has a value close to the temperature of the lower troposphere. And it is defined,

$$T_{mean} = \frac{\int_{z_1}^{z_t} T(z) \alpha(z, \nu) e^{-\tau(z, \nu)} dz}{\int_{z_1}^{z_t} \alpha(z, \nu) e^{-\tau(z, \nu)} dz} \quad (1)$$

Author’s changes in the manuscript: Page 7, line 147

~~T_{mean} is the temperature at approximately 2.5 km altitude of the actual temperature profile approaching exponentially the surface value (Peter, 1997).~~ [depends upon the temperature profile as well as on the absorption profile at a specific frequency. Since the number density is highest at low altitudes and the absorption is highest near the ground, \$T_{mean}\$ has a value close to the temperature of the lower troposphere \(Ingold *et al.*, 1998\).](#)

6. **Comments from the referee:** Pg. 16379, around line 10: I would argue that 5% difference are not a “small” bias, when you try to analyse 3% per decade trends. As mentioned, I find it disappointing that no other instruments (lidars, satellites) were used as independent references.

Author’s response:

As we highlighted previously, mean relative differences of GROMOS-FFTS and independent data sets (lidar, satellites and ozonesondes) are less than 10% between 50 and 0.1 hPa.

Author’s changes in the manuscript: Page 9, line 208

The purpose of the harmonisation is to correct this ~~small~~-bias between both spectrometers, by using the data from FFTS as reference.

7. **Comments from the referee:** Pg. 16380, line 14: Where do the 7.2 and 8.4 months come from? Please mention (e.g. 8.4 and 24 months are the annual modulation sidebands of a 28 month QBO)

Author’s response:

7.2 and 8.4 months are the annual modulation sidebands of 18 and 28 months oscillation respectively, both related with QBO.

Author’s changes in the manuscript: No changes.

8. **Comments from the referee:** Pg. 16380, line 24: Where does the error covariance matrix come from? Are the diagonal elements from your error/ uncertainty considerations in Section 5? Where do the off-diagonal elements come from? Are they from the various lag-auto-correlations of the residuals after the regression? Are they significant? How big is the effect of the off-diagonal elements? Please make this part a lot clearer.

Author’s response:

The diagonal elements of the error covariance matrix are the uncertainty of the ozone monthly mean profiles, described in Section 5 Uncertainty considerations. The off-diagonal elements are initially set zero. In a second iteration, the correlation coefficients between each data-point and its nth neighbour are estimated from the fit residuals, and an additional error term is built, based on these covariances, describing the deficiency of the multi-parametric model chosen. This error term (in terms of covariance matrix) is scaled according to chi-square statistics and added to the initial measurement error covariance matrix.

Author’s changes in the manuscript: Page 12, line 242

~~; with the squared standard errors of the monthly means as the diagonal terms (?). The autocorrelations among data points are considered in the covariance matrix, and a model error component is assessed iteratively and added to the covariance matrix in order to account the autocorrelative nature of the atmosphere and to get realistic error estimates.—~~ The diagonal elements of the error covariance matrix are the uncertainty of the ozone monthly mean profiles, described in the following section. The off-diagonal elements are initially set zero. In a second iteration, the correlation coefficients between each data-point and its nth neighbour are estimated from the fit residuals, and an additional error term is built, based on these covariances, describing the deficiency of the multi-parametric model chosen. This error term (in terms of covariance matrix) is scaled according to chi-square statistics and added to the initial measurement error covariance matrix.

9. **Comments from the referee:** Pg. 16381 1st paragraph: As mentioned, the shape

of the residuals in Fig. 6 (middle panel) suggests strongly that a quadratic term should also be included/ tested in Eq. 1.

Author’s response:

As previously mentioned, we think that there is no physical argument for adding a quadratic term in the trend model. The shape of the residuals at 10 hPa shows some short term anomalies.

Author’s changes in the manuscript: No changes.

10. **Comments from the referee:** Pg. 16381, lines 7-8: “Most ... can be explained”. Please be more quantitative. What fraction of the variance is explained? What are typical values for R^2 ?

Author’s response:

No comments.

Author’s changes in the manuscript: Page 13, line 259

The residual is within 0.5 ppmv except for some particular cases. ~~Most of the ozone variations can be explained by the fitted proxies~~, maybe due to some short term anomalies.

11. **Comments from the referee:** Pg. 16382: Eqs. 2 and 3 are not correct. There needs to be a square root taken from $\frac{1}{n-1} \sum$ on the right side.

Author’s response:

No comments.

Author’s changes in the manuscript: Page 14, eqs. 2 and 3

$$\sigma = \frac{1}{n-1} \sum_{i=1}^n (x_i - \bar{x})^2 \sqrt{\frac{1}{n-1} \sum_{i=1}^n (x_i - \bar{x})^2} \quad (2)$$

$$SEM = \frac{\sigma}{\sqrt{DGF}} = \frac{1}{(n-1)\sqrt{DGF}} \sum_{i=1}^n (x_i - \bar{x})^2 \frac{1}{\sqrt{(n-1)DGF}} \sqrt{\sum_{i=1}^n (x_i - \bar{x})^2} \quad (3)$$

12. **Comments from the referee:** Pg. 16383, last paragraph: Why are the data from 1994 to 1997 not used? This should be mentioned, and should be explained.

Author’s response:

As we mentioned on Section 6: Results and discussion, the selection of the time interval is based on the assumption that 1997 is the turn-around year of EESC. Therefore, we decided to discard the firsts years of GROMOS measurements in order to not bias the trend result by starting before the EESC peak at mid-latitudes.

Author’s changes in the manuscript: No changes.

13. **Comments from the referee:** Pg. 16384, line 14: Which studies? The ones below? Please reword/ clarify.

Author’s response:

No comments.

Author's changes in the manuscript: Page 16, line 338

On the other hand, other recent studies

([Eckert et al., 2014](#); [Vigouroux et al., 2015](#); [Harris et al., 2015](#); and references therein)

have found positive but not significant trend in our location. But we have to be careful about these discrepancies since it could arise from differences in treatment and propagations of uncertainties, selection of data, ozone measurement techniques, statistical approach, latitudinal and altitudinal extent and/or the time period covered in the trend study (~~[Eckert et al., 2014](#); [Vigouroux et al., 2015](#); [Harris et al., 2015](#); and references therein~~).

14. **Comments from the referee:** Pg. 16385, line 17 to page 16386, line 10: This discussion has little to do with the presented GROMOS data and is not supported by anything else presented in the paper. As such is speculative and I strongly suggest that it should simply be deleted.

Author's response:

The aim of this discussion is to present to the reader a wider view of stratospheric ozone, considering the ozone photochemistry and transport processes along with anthropogenous and natural changes of the global circulation system. Changes in the position and strength of the circulation cells may induce regional changes in ozone. A discussion of this topic is important for our article since it underlines the need for reliable monitoring and detection of ozone trends over the next decades.

Author's changes in the manuscript: No changes.

15. **Comments from the referee:** Pg. 16386, lines 11 to 16: What is the explanation for the declining ozone trend in the mesosphere? Please add an explanation.

Author's response:

Unfortunately no explanation so far have been given in the literature for such a decline of ozone in the mesosphere though several other authors observed the same effect as mentioned in Section 6: Results and discussion. The mesospheric ozone trend would be an interesting topic for a simulation study with a chemistry climate model such as WACCM.

Author's changes in the manuscript: No changes.

16. **Comments from the referee:** Pg. 16391, line 6, Typo: temporal

Author's response:

No comments.

Author's changes in the manuscript: Page 22, line 525

Tiao, G. C., Reinsel, G. C., Xu, D., Pedrick, J. H., Zhu, X., Miller, A. J., DeLuisi, J. J., Mateer, C. L., and Wuebbles, D. J.: Effects of autocorrelation and ~~tempotal~~ [temporal](#) sampling schemes on estimates of trend and spatial correlation, *J. Geophys. Res.*, 95, 20507-20517, doi:10.1029/JD095iD12p20507, 1990

17. **Comments from the referee:** Figure 4: I do not find this plot useful. Mostly it shows repetition of the well known annual cycle. To make this plot useful, it would be much much better to remove the annual cycle and show ozone anomalies, either as ppmv or as % deviation from the annual cycle. Please make a better plot.

Author’s response:

The reason to include this harmonised 20 years time series of stratospheric ozone VMR profiles, is to show our harmonised data prior the trend analysis. This figure surely shows the annual cycle but also the increase (positive anomaly) of mid-stratospheric ozone in last years. Further, with this figure one can get a view of the maximum of ozone at our station and its evolution over the last two decades.

Author’s changes in the manuscript: No changes.

18. **Comments from the referee:** Figure 7: I think this Figure could be improved a lot by not comparing apples (=%) and eggs (ppmv and days). The total uncertainty (blue line) should not be shown in ppmv, but also in percent. Then it becomes comparable with the estimated (thermal) observation noise (purple line), and with the observed uncertainty (black line). Instead of time lag (red line) the $1/\sqrt{DGF}$, converted also to % of the ozone profile, should be shown. I would expect that this atmospheric variability part would explain why the observed uncertainty is much larger than the thermal noise at levels between 100 hPa and 10 hPa. These changes would result in a much clearer plot.

Author’s response:

We agree with the referee that all the uncertainties should be shown in percent. Regarding the monthly mean correlation length profile we believe that this should be shown in units of days. Anyway, even showing it in units of days one can easily estimate the DGF from the correlation length profile. For example, if the amount of measurements of GROMOS within a month is around 1300, and at 10hPa the time lag is around 2 days then the DGF are more or less 12.5. Following the same assumption, at 100 hPa (time lag around 5 days) the DGF are 4.8 and 81.25 at 1hPa (8 hours of time lag).

Author’s changes in the manuscript: Page 15, line 312, Figure 8

Figure ~~??-1~~ shows the error budget used as input for the trend estimation model. The red line is an example of monthly mean correlation length profile, in day units, calculated for the time interval from October 2011 to October 2014. We can see the monthly autocorrelations of stratospheric ozone. The magenta line is the monthly mean observation error profile, from the thermal noise on the spectra, calculated for the same time interval. The ~~black-blue~~ line is the estimated ~~systematic-instrumental~~ error profile based on recent and past intercomparisons of coincident data from GROMOS, ozonesondes, nearby lidars and satellites. And the ~~blue-line represents in ppm-VMR~~-black line represents the total contribution of the uncertainty of GROMOS taking into account all the aforementioned errors.

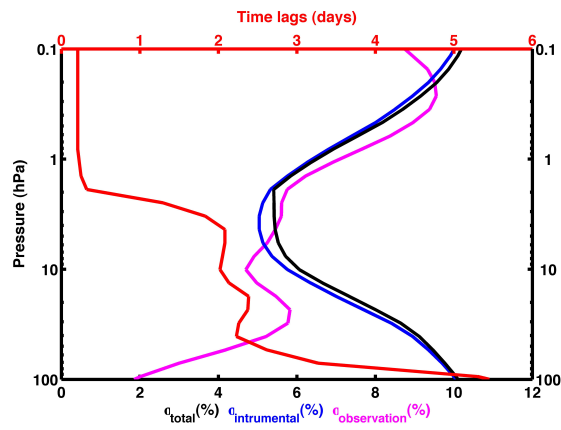


Figure 1: Uncertainty budget of GROMOS used in the trend analysis. The red line is an example of monthly mean correlation length profile, in day units, calculated for the time interval from October 2011 to October 2014. The magenta line is the monthly mean observation error profile, calculated for the same time interval. The ~~black-blue~~ line is the estimated ~~systematic-instrumental~~ error profile. And the ~~blue-black~~ line represents ~~in ppm-VMR~~ the total contribution of the uncertainty of GROMOS.

Response to anonymous referee #2

Lorena Moreira

August 27, 2015

We would like to thank the Referee #2 for the careful reading of our manuscript and for giving constructive comments which substantially helped to improve the quality of the paper. All proposed objections and suggestions have been taken into account and discussed. Below we try to answer every comment.

Specific comments

1. **Comments from the referee:** Section 1: Introduction

A summary of the historical use of ground-based microwave measurements to detect ozone trends is missing. Reading the present paper, it seems that no study has been made about this except for the Dumitru et al. (2006) paper. But microwave measurements from several stations have been used in the WMO (2014) report. How the present study fits in this context? Is it the same methodology that is used for the Bern station in WMO (2014)? And what about the other stations used in WMO (2014)? Any other publications,...

Author's response:

Regarding the historical use of ground-based microwave measurements to detect ozone trends what we have found on the literature are Steinbrecht *et al.* (2006 and 2009) and the WMO (2014). In fact, since Steinbrecht *et al.* (2006) we are not aware of any other ozone trend study based on ground-based microwave measurements, therefore, the purpose of this paper is to present a new trend estimation based on stratospheric ozone profiles measured by a ground-based microwave radiometer at northern midlatitudes.

As mentioned in Section 6: Results and discussion, our trend result is in agreement with those reported in WMO (2014). The WMO (2014, Table 2.4) reported a statistically significant ozone increase of (3.9 ± 1.3) (% decade⁻¹) at 40 km in the upper stratosphere at northern mid-latitudes (35-60 °N) over the 2000-2013 period. This ozone trend value is based on observations from various space-based and ground-based measurement instruments. A slightly different ozone series of the GROMOS instrument contributed to the ozone trend estimation of WMO (2014). The ozone trend of our study cannot be directly compared to WMO (2014) since the method of trend determination, the time window and the measurement region differ. However, the ozone trend at Bern (about 3.0%/decade at 40 km) agrees well with the ozone trend at northern mid-latitudes (about 3.9%/decade at 40 km) as reported by WMO (2014).

Author's changes in the manuscript: Page 2, line 47

~~Ozone time series from the GROMOS microwave radiometer were used to assess the stratospheric ozone trend above Bern and for validation of satellite observations (Dumitru *et al.*, 2006~~ The concerns regarding anthropogenic depletion of stratospheric ozone increased the necessity for precise and accurate measurements to monitor long term trend in this specie. (Parrish *et al.*, 1992). Passive millimeter wave radiometry has been used to monitor the vertical distribution of atmospheric trace gases since the early 1970s (Parrish *et al.*, 1992). The need for continuous monitoring of the stratospheric response to anthropogenic trace gas releases, performed by a well defined set of instruments, led to the foundation of the Network for the Detection of Stratospheric Change (NDSC) (now Network for the Detection of Atmospheric Composition Change - NDACC) in 1991. The ozone radiometer GROMOS is part of the NDACC, hence our entire dataset is available via <http://ftp.cpc.ncep.noaa.gov/ndacc/station/bern/hdf/mwave/> Ozone time series from the GROMOS microwave radiometer were used for comparisons with lidar, ozonesondes and collocated satellite observations and for detection of long-term trends (Dumitru *et al.*, 2006; Steinbrecht *et al.*, 2006; Steinbrecht *et al.*, 2009; Keckhut *et al.*, 2010; van Gijssel *et al.*, 2010; Studer *et al.*, 2013; Delcloo and Kreher, 2013; WMO, 2014).

Page 3, line 80

... with a representative station in central Europe. Trend studies of ozone profiles based on ground-based microwave measurements are rare. In fact, since Steinbrecht *et al.*, 2006 we are not aware of any other publication, therefore, the purpose of this paper is to present a new trend estimation based on stratospheric ozone profiles measured by a ground-based microwave at northern midlatitudes (46.95°N, 7.44°E, 577 m). The present study is organised as follows: ...

2. Comments from the referee: Section 2.3: Retrieval procedure (p.16376-16378)

I recommend to include more details on the characterization of the ozone profiles obtained with the OEM:

- a) OEM requires the use of a priori information, which includes a priori profile (discussed in the paper) but also a priori covariance matrix which is not mentioned in the paper. Can the authors provide this missing information?
- b) The authors provide in the text the vertical resolution in the stratosphere (8-12km) and lower mesosphere (20-25km), but the reader would have a more global picture with the knowledge of the numbers of degrees of freedom for signal and a plot of the averaging kernels as often provided when OEM is used. This would help to interpret Fig.8, underlying the fact that the actual knowledge of the vertical structure of the ozone trends is much less than what a reader could interpret from the trend profile in Fig. 8. Also, for information, how much of the a priori contributes outside of the 20
- c) Errors: the smoothing error values (in function of altitude) should also be provided. The link between the errors discussed in this section (2.3) and the uncertainties in Section 5 is not clear. Do I understand well that the error budget provided by OEM (l.9, p.16377) is not used in the “uncertainty analysis” section?

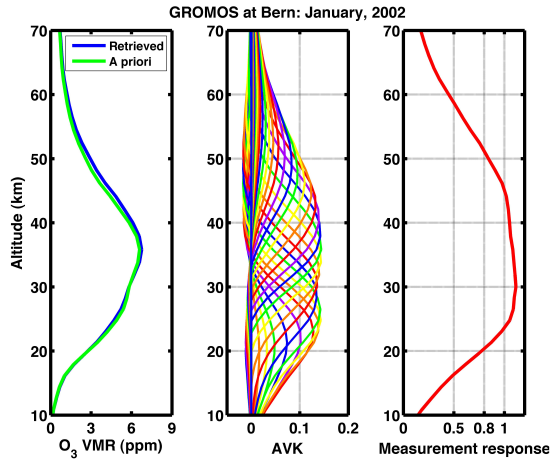


Figure 1: Example of an a priori profile and a retrieved ozone profile (left panel), averaging kernels (middle panel) and the measurement response (area of averaging kernels) (right panel) of the GROMOS retrieval for January, 2002

Author's response:

a) As diagonal elements of the a priori covariance matrix we assume a relative error around 35% at 100 hPa. The error decreases in the lower stratosphere up to 28%. Then it increases linearly from 35% in the upper stratosphere to 70% in the lower mesosphere. The off-diagonal elements exponentially decrease with a correlation length of 3 km.

b) Figure 1 shows an example of an a priori profile (green line) and retrieved ozone profile (blue line) in the left panel, the averaging kernels (AVKs) (matrix columns in (ppmv/ppmv)) in the middle panel and in the right panel the measurement response (area of averaging kernels) of the GROMOS retrieval for January, 2002. An estimate of the a priori contribution to the retrieval can be obtained by the area of the averaging kernels (measurement response). Between 20 to 52 km (50 to 0.5 hPa) the measurement response (right panel in Figure 1) is higher than 0.8 what corresponds to an a priori contribution less than 20%. Consequently, the retrieved ozone values at these altitudes are predominantly based on the measured line spectrum.

c) As described in Subsection 2.3: Measurement principle and retrieval procedure, the total error provided by the OEM during the retrieval procedure includes systematic error, random error and the smoothing error. The systematic error originates from the tropospheric correction, calibration error due to systematic error in the load temperatures, errors due to baseline features, spectral parameter, etc. The smoothing error is caused by the low altitude resolution of the data retrieved from the measurements; hence smoothing error is almost time-independent in size and sign, i.e. is an almost constant error. We do not consider any kind of systematic error during the trend analysis since they cancel out, thus, it does not have any impact on the trend analysis. Accordingly, the only contribution from the

OEM error budget to the uncertainty analysis in Section 5 is the random error. The random error is mainly due to the propagation of the thermal noise of the brightness temperature into the ozone profile. In Section 5 we recall this random error as observation uncertainty.

Author’s changes in the manuscript: Page 7, line 160

The vertical resolution depends upon altitude and can be estimated from the full width at half maximum (FWHM) of a kernel line. The averaging kernels (AVK) and the area of the averaging kernels (AoA) of GROMOS are shown on the middle and right panel of Figure 1. For GROMOS the vertical resolution lies generally within 8-12 km in the stratosphere and increases with altitude to 20-25 km in the lower mesosphere. ~~In the case of GROMOS, the ozone VMR profiles are retrieved with less than 20% of~~ An estimate of the a priori contribution ~~from 30 to 0.3 hPa (altitudes from about 25 to 57 km).~~ to the retrieval can be obtained by the area of the averaging kernels (measurement response). Between 20 to 52 km (50 to 0.5 hPa) the measurement response is higher than 0.8 what corresponds to an a priori contribution less than 20%. Consequently, the retrieved ozone values at these altitudes are predominantly based on the measured line spectrum.

Page 8, line 172

~~-As diagonal elements of the a priori covariance matrix we assume a relative error around 35% at 100 hPa. The error decreases in the lower stratosphere up to 28%. Then it increases linearly from 35% in the upper stratosphere to 70% in the lower mesosphere. The off-diagonal elements exponentially decrease with a correlation length of 3 km.~~

3. Comments from the referee: Section 3: Harmonization strategy for the ozone profiles and Fig.3

a) Fig.3 left panel: the authors show the mean of the profiles obtained from the 2 instruments during the same period. And the blue dashed lines are the error on the FFTS instrument. This error is “the total error from the retrieval along with the error from natural variability of FFTS for this time”: is it relevant to include the error “from natural variability” (note that this error is not very clear in this section and only explained in Sect. 5), since both instruments are measuring at the same time and since therefore the natural variability should be the same in both cases? Secondly, is it the total error of an individual measurement or the total error on the mean profile (random errors divided by the square root of the number of measurements) which would be more relevant since this plot compares means of profiles?

b) Fig.3 middle panel: “...presents the mean relative difference profile between data of both spectrometers...” It is not clear if it is the difference between the two profiles shown in the left panel (means of the profiles), or if it is the mean of the individual differences between 2 measurements (collocated in time). Please, clarify. The latter is usually used for assessing bias between instruments. Using the former method could lead to wrong bias assessment (e.g. the difference on the 2 means could come from few outliers in one of the 2 data sets means), while the other individual collocated measurements would be in agreement. When the latter

method is used, one can conclude if the bias is significant or not looking at the statistical standard deviation of the individual differences. From the figure (middle panel), it gives the impression that the bias is not significant because of the grey dashed lines (error on one single FFTS measurements or on the mean profile?) being larger than the difference. If this is true, why correcting for a bias if it is not significant? How looks your Fig. 8 if you do not make the bias correction? I suggest to plot the mean of the relative differences between individual measurements and the error on that mean (using the standard deviation of the statistics) in Fig.3, middle panel (and right panel), and conclude about the significance of the bias between the 2 instruments.

Author’s response:

In accordance with the referee wishes, we have changed Fig.3. In Figure 2 we have represented in the left panel the mean ozone profiles recorded by FB (red line) and by FFTS (blue line) for the Oct.2009-Aug.2011 time interval. The dashed lines are the standard deviations of the measurements. In the middle panel we have plotted the mean of the relative differences between individual measurements. The dashed line is the standard deviation of the differences. Finally in the right panel is presented the mean absolute difference profile used to harmonise the GROMOS data set.

Author’s changes in the manuscript: Page 9, line 199, Figure 4

In Figure 32, we show in the left panel the mean ozone profiles recorded by FB (red line) and by FFTS (blue line), for this time interval. The ~~blue~~ dashed lines are the ~~total error from the retrieval along with the error from the natural variability of FFTS for this time interval. As we are using FFTS data as reference for the FB data and in order to make the figure more straightforward we only show the error profile from FFTS~~ standard deviation of the measurements. The middle panel presents the mean relative difference profile between data of both spectrometers with the FFTS data as reference. The ~~grey dashed lines delimit the FFTS error centred at zero~~ dashed line is the standard deviation of the differences.

4. Comments from the referee: Trend estimation method

- a) Choice of the von Clarmann et al. (2010) method: can the authors explain more what is the benefit of using this method compared to the “traditional” one (i.e. without using a full error covariance matrix) which corrects the trend uncertainties for the autocorrelation in the residuals by using a Cochrane-Orcutt transformation to the model (e.g. in Brunner et al., ACP 2006; Chehade et al., ACP 2014; Coldewey-Egbers GRL, 2014; ...) or by simply applying a correction in the uncertainty (e.g. Nair et al., ACP, 2013; ...)? Does the von Clarmann et al. (2010) method impact also the trends themselves or only the uncertainties on the trends?
- b) It seems that 7 harmonics is much more than what is usually found in the literature (e.g. from 2 to 4 harmonics are found in the references given above). Does it improve significantly the residuals and the coefficient of determination (R^2) to add harmonics? What was the criteria to choose 7 harmonics?
- c) The ENSO signal in Fig. 6 seems very low: is the parameter “f” (in Eq. 1) significant? If not why not remove it from the model?
- d) Other proxies (e.g. Northern Atlantic Oscillation; eddy heat flux,...) can also be used in ozone trend studies (Weber et al., ACP, 2011; Frossard et al., ACP,

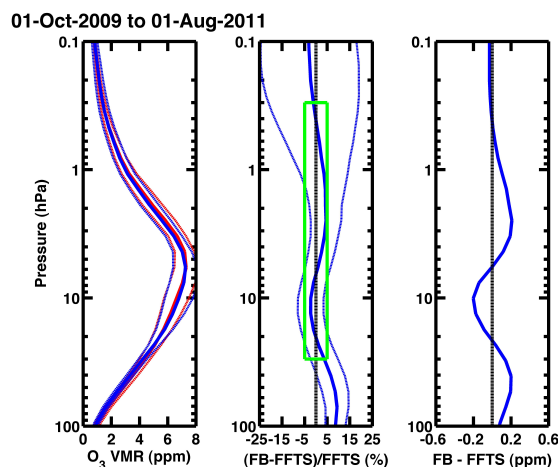


Figure 2: Harmonisation of ozone profiles retrieved from the FB (red line in the left panel) and FFT (blue line in the left panel) spectrometers. The bias between FB and FFTS is less than 5% (middle panel) as derived from the overlap measurement (2009 to 2011) of ozone profiles at pressure levels from 30 to 0.3 hPa (valid altitude range of GROMOS, green box). The blue dashed lines and the grey dashed lines represent the error of FFTS

2013;...). Any reason not to include them? Were they tested and found not significant?

e) The plot of the residuals (Fig.6) rises a question: do you have an explanation for the observed oscillation in the residuals?

f) Since the authors provide a trend profile (Fig.8), it could be useful to add the proxies contribution as a function of altitude as well, and to include the information about their significance (as a function of altitude).

Author's response:

a) The advantage is that a scheme which supports the use of the full covariance matrix can solve multiple problems having to do with covariances: (a) model deficiencies which go along with auto-correlated residuals (b) correlated measurement errors (c) biases between data subsets. For particular applications the methods mentioned may be equally well suited but the von Clarmann's approach offers a tool which serves multiple purposes. Indeed the trend itself can change. This is because the algorithm supports weighting of the data points according to their data errors. By adding the covariance term (which assigns the same model error to each data point), the weight of the data points will change. The contrast of the weights will become smaller.

b) Other publications using the von Clarmann *et al.* (ACP, 2010) method also employ 8 harmonics (Eckert *et al.* (ACP, 2014); Stiller *et al.* (ACP, 2012); Kellmann *et al.* (ACP, 2012)). As mentioned in Section 4: Trend estimation method, the selection of the harmonics was done based on the power spectra of GROMOS time series.

c) The ENSO signal, as you can see in Fig.6, is useful to take into account the

effect of ENSO 1997.

d) Due to the von Clarmann et al. (2010) method is a novel trend estimation program it has not been tested for all the proxies yet.

e) The shape of the residuals at 10 hPa shows some short term anomalies, maybe due to some regional variation not included in the trend method. In addition, one cannot expect that the series of the climate indices are sufficient to represent the natural variability of the Earth system completely.

f) In Fig.6 is represented the ozone fitted signals of the proxies QBO, solar F10.7 cm flux and ENSO at 10 hPa. Nevertheless, we consider that the study of the contribution of the proxies to the ozone variability is beyond the work of this linear trend paper. Further, it is planned a separate and detailed study of the natural variations of ozone due to these oscillations.

Author's changes in the manuscript: No changes.

5. **Comments from the referee:** Uncertainty considerations

a) I don't understand why in the second type of error ("observation error"), the authors just use the thermal noise error instead of the full random error budget from OEM (thermal noise + smoothing + maybe other random sources).

b) The authors consider a systematic error using validations studies: I would guess that a (constant) systematic error should not impact the trends. Instead, I would investigate for a possible drift in your time-series by using the validation results. This would enlarge the trend uncertainties.

Author's response:

a) As indicated previously, in the answer of the referee's comment number 2 c), we do not consider systematic error contributions during the trend estimation.

b) In order to avoid misunderstandings we should rename this systematic error as instrumental error. In this instrumental uncertainty we assume an uncorrelated monthly instrumental error of about 5 to 10% for GROMOS. The reason to enlarge the GROMOS uncertainty by adding this instrumental uncertainty is to be on the safe side during the trend uncertainty estimation. The large number of GROMOS measurements per month (an ozone profile each 30 minutes) allows a robust assessment of the uncertainty from natural variability. But in turn this large number of measurements lead to a small contribution due to the error of the natural variability. From past cross-validations of GROMOS with collocated instruments we know that the different instruments and measurement techniques can differ by 5-10%. Sometimes, these biases may change with month, season or year. This behaviour of the biases might be due to the sophisticated measurement and retrieval techniques.

Author's changes in the manuscript: Page 14, line 298

Finally, ~~owing the fact that we had not taken into account any kind of systematic uncertainty of the instrument, we have chosen to include as uncertainty source an~~

~~estimation of systematic error profile~~ we assume an uncorrelated monthly instrumental uncertainty. The aim is to take into account the bias between GROMOS and other instruments, and thereby to get a realistic uncertainty estimation.

6. **Comments from the referee:** Results and discussion

Any explanation for the negative trend in the lower mesosphere? You checked your results with other experimental studies: are there available modelling studies that could help you to explain this trend?

Author's response:

In Section 6: Result and discussion it is mentioned that this lower mesospheric negative ozone trend was also reported in recent trend estimations (Tummon *et al.* (ACP, 2015); Remsberg *et al.* (ACP, 2014); Kyrölä *et al.* (ACP, 2013)) but what would be the origin of this effect would have to be investigated in a separate project.

Author's changes in the manuscript: No changes.

Minor or technical comments

1. **Comments from the referee:** p.16372, 1.4 (abstract): Provide longitude and latitude of the instrument. Also in p. 16374, 1.13.

Author's response:

No comments.

Author's changes in the manuscript: Page 1, line 3

The ozone radiometer GROMOS (GROUND-based Millimeterwave Ozone Spectrometer) performs continuous observations of stratospheric ozone profiles since 1994 above Bern, Switzerland (46.95°N, 7.44°E, 577 m).

Page 3, line 68

Among other advantageous technical features, the 20 years of continuous observations and the privileged location of the instrument offer us a pretty clear vision of the distribution of ozone in the northern mid-latitudes (46.95°N, 7.44°E, 577 m).

2. **Comments from the referee:** p.16372, 1.20-22 (abstract): Provide the corresponding approximate altitudes for the trends at 4.36hPa and 02.hPa.

Author's response:

No comments.

Author's changes in the manuscript: Page 1, line 17

With our observed ozone profiles, we are able to support this statement by reporting a statistically significant trend of +3.14 % decade⁻¹ at 4.36 hPa (37.76 km), covering the period from January 1997 to January 2015, above Bern. Additionally, we have estimated a negative trend over this period of -3.94 % decade⁻¹ at 0.2 hPa (59 km).

3. **Comments from the referee:** p.16373, 1.4-6: Not clear to me. "...ozone losses were 15-18

Author's response:

We delete this sentence.

Author's changes in the manuscript: Page 2, line 27

~~Early predictions of ozone losses were 15 -- 18% if CFCs added 5.5 -- 7.0 ppbv of chlorine to the stratosphere at 1975 rates (Hudson and Reed, 1979). Thereafter, these were confirmed in many publications, such as in the~~ In the last Scientific Assessment of Ozone Depletion: 2014 of the World Meteorological Organisation (WMO, 2014) ~~, where it~~ is stated that global ozone levels decreased through the 1980s and early 1990s while stratospheric abundances of ozone depleting substances (ODS) were increasing.

4. **Comments from the referee:** p.16375, l. 5: "And" instead of "An".

Author's response:

No comments.

Author's changes in the manuscript: Page 3, line 90

~~An~~ And finally, Section 7 is a summary of our findings.

5. **Comments from the referee:** p. 16381, l. 8: the "." is missing at the end.

Author's response:

No comments.

Author's changes in the manuscript: Page 13, line 259

~~Most of the ozone variations can be explained by the fitted proxies,~~ maybe due to some short term anomalies.

6. **Comments from the referee:** p.16381, l.12: "...we have considered 3 different ways to assess the uncertainties": this gives the impression that you will then choose between the 3, while at the end you sum them. So change to something like "We have considered 3 types of errors".

Author's response:

No comments.

Author's changes in the manuscript: Page 13, line 264

We have considered three ~~different ways to assess the~~ types of uncertainties.

7. **Comments from the referee:** p.16395, legend Fig3.: "...30 to 0.5 hPa": should be 0.3hPa, according to the text and the green box.

Author's response:

No comments.

Author's changes in the manuscript: Page 8, caption Figure 3

Caption Figure 3: Harmonisation of ozone profiles retrieved from the FB (red line in the left panel) and FFT (blue line in the left panel) spectrometers. The bias between FB and FFTS is less than 5% (middle panel) as derived from the overlap measurement (2009 to 2011) of ozone profiles at pressure levels from 30 to ~~0.5~~ 0.3 hPa (valid altitude range of GROMOS, green box). The blue dashed lines and the grey dashed lines represent the error of FFTS

Trend analysis of the 20 years time series of stratospheric ozone profiles observed by the GROMOS microwave radiometer at Bern

L. Moreira¹, K. Hocke¹, E. Eckert², T. von Clarmann², and N. Kämpfer¹

¹Institute of Applied Physics and Oeschger Centre for Climate Change Research, University of Bern, Bern, Switzerland

²Karlsruhe Institute of Technology, Institute for Meteorology and Climate Research, Karlsruhe, Germany

Correspondence to: L. Moreira (lorena.moreira@iap.unibe.ch)

Abstract. The ozone radiometer GROMOS (GROund-based Millimeterwave Ozone Spectrometer) performs continuous observations of stratospheric ozone profiles since 1994 above Bern, Switzerland ([46.95°N, 7.44°E, 577 m](#)). GROMOS is part of the Network for the Detection of Atmospheric Composition Change (NDACC). From November 1994 to October 2011, the ozone line spectra were measured by a filter bench (FB). In July 2009, a Fast-Fourier-Transform spectrometer (FFTS) has been added as backend to GROMOS. The new FFTS and the original FB measured in parallel for over two years. The ozone profiles retrieved separately from the ozone line spectra of FB and FFTS agree within 5% at pressure levels from 30 to 0.5 hPa, from October 2009 to August 2011. A careful harmonisation of both time series has been carried out by taking the FFTS as the reference instrument for the FB. This enables us to assess the long-term trend derived from more than 20 years of stratospheric ozone observations at Bern. The trend analysis has been performed by using a robust multilinear parametric trend model which includes a linear term, the solar variability, the El Niño - Southern Oscillation (ENSO) index, the quasi-biennial oscillation (QBO), the annual and semi-annual oscillation and several harmonics with period lengths between 3 and 24 months. Over the last 15 years, some experimental and modelling trend studies have shown that the stratospheric ozone trend is levelling off or even turning positive. With our observed ozone profiles, we are able to support this statement by reporting a statistically significant trend of +3.14 % decade⁻¹ at 4.36 hPa ([37.76 km](#)), covering the period from January 1997 to January 2015, above Bern. Additionally, we have estimated a negative trend over this period of -3.94 % decade⁻¹ at 0.2 hPa ([59 km](#)).

20 1 Introduction

For many decades it is known that the stratospheric ozone layer shields the Earth's surface from harmful solar ultraviolet radiation (UV), thus enabling life on Earth and protecting humans and the biosphere against adverse effects. Molina and Rowland (1974) were the first to propose that this protective layer could be depleted by anthropogenic emission of chlorofluorocarbons (CFCs) to the atmosphere. The photodecomposition of CFCs and other long-lived organic molecules in the stratosphere releases chlorine (Cl) and bromine (Br) atoms that destroy ozone molecules in catalytic cycles. ~~Early predictions of ozone losses were 15–18% if CFCs added 5.5–7.0 ppbv of chlorine to the stratosphere at 1975 rates (Hudson and Reed, 1979). Thereafter, these were confirmed in many publications, such as in the~~ In the last Scientific Assessment of Ozone Depletion: 2014 of the World Meteorological Organisation (WMO, 2014) ~~, where it~~ is stated that global ozone levels decreased through the 1980s and early 1990s while stratospheric abundances of ozone depleting substances (ODS) were increasing.

In 1985, massive ozone losses in measured column abundances during the Antarctic spring were reported and heterogeneous chlorine chemistry on polar stratospheric clouds (PSCs) were implicated for the loss (WMO, 2011). Around that time and over the later years, the Montreal Protocol and its amendments and adjustments were enacted with the aim to reduce the production and consumption of ODSs. Actions taken under the Montreal Protocol have led to decreases in the atmospheric abundance of controlled ODSs, and are enabling the return of the ozone layer toward 1980 levels (WMO, 2014).

From the late 1990s, there were some measurements and model calculations indicating a turnaround in the decreasing ozone, suggesting that the negative ozone trends in the stratosphere would level out or even become positive (Huang *et al.*, 2014); Newchurch *et al.*, 2003). Nevertheless, during this recovery phase, ozone levels will also be affected by the expected anthropogenic increases in abundances of other ozone-relevant gases (carbon dioxide (CO₂), methane (CH₄), and nitrous oxide (N₂O)) as well as by the natural influences of volcanic eruptions, solar activity, and the natural variability in the Earth's climate (WMO, 2014).

~~Ozone time series from the GROMOS microwave radiometer were used to assess the stratospheric ozone trend above Bern and for validation of satellite observations (Dumitru *et al.*, 2006~~ The concerns regarding anthropogenic depletion of stratospheric ozone increased the necessity for precise and accurate measurements to monitor long term trend in this specie. (Parrish *et al.*, 1992). Passive millimeter wave radiometry has been used to monitor the vertical distribution of atmospheric trace gases since the early 1970s (Palm *et al.*, 2010). The need for continuous monitoring of the stratospheric response to anthropogenic trace gas releases, performed by a well defined set of instruments, led to the foundation of the Network for the Detection of Stratospheric Change (NDSC) (now Network for the Detection of Atmospheric Composition Change - NDACC) in 1991. The ozone radiometer GROMOS is part of the NDACC , hence our more than 20 years harmonised time series are available

via <http://ftp.cpc.ncep.noaa.gov/ndacc/station/bern/hdf/mwave/>

[Ozone time series from the GROMOS microwave radiometer were used for comparisons with lidar, ozonesondes and collocated satellite observations and for detection of long-term trends \(Dumitru *et al.*, 2006 ;](#)

60 [Steinbrecht *et al.*, 2006 ; Steinbrecht *et al.*, 2009 ; Keckhut *et al.*, 2010 ; van Gijssels *et al.*, 2010 ; Studer *et al.*, 2013 ; Delcloo and Kreher, 2013 ; WMO, 2014 \).](#)

Ground-based millimeter wave radiometry is a powerful technique for trace gas measurements due to its low sensitivity to weather conditions and aerosol contamination. Since ozone radiometers measure the thermal microwave emission of ozone in the middle atmosphere, they do not require external
65 illumination sources, such as laser pulses or the solar irradiance. The measurements can therefore be made throughout day and night. Among other advantageous technical features, the 20 years of continuous observations and the privileged location of the instrument offer us a pretty clear vision of the distribution of ozone in the northern mid-latitudes ([46.95°N, 7.44°E, 577 m](#)).

We perform a trend study of our 20 years time series of stratospheric ozone profiles through a new
70 robust multilinear parametric trend estimation method (von Clarmann *et al.*, 2010). The program minimises a cost function in order to estimate the linear trend of a time series. The cost function consists of the quadratic norm of the residual between a regression model and the measured time series, weighted by the inverse covariance matrix of the data errors. Error correlations between data points are supported, making the program suitable for consideration of auto-correlated residuals.

75 The regression model consists of an axis intercept, a linear trend, ~~harmonic variations~~[sine waves](#), and several proxies. Unknown biases between data subsets are handled by assigning a fully correlated error term to each data point of one of the data subsets. With this trend analysis tool a complete treatment of the uncertainties is assured, making this trend analysis particularly valuable to confirm the aforementioned ozone turnaround with a representative station in central Europe.

80 [Trend studies of ozone profiles based on ground-based microwave measurements are rare. In fact, since Steinbrecht *et al.*, 2006 we are not aware of any other publication, therefore, the purpose of this paper is to present a new trend estimation based on stratospheric ozone profiles measured by a ground-based microwave at northern midlatitudes \(46.95°N, 7.44°E, 577 m\).](#)

85 The present study is organised as follows: the description of the instrument, the measurement technique, the spectrometer upgrade and the retrieval method are presented in Section 2. Section 3 summarises the procedure carried out for the harmonisation of ozone profiles, followed by a detailed description of the trend estimation method in Section 4. Section 5 deals the characterisation of GROMOS uncertainty sources. The estimated trend is presented in Section 6, concluding with an
90 overview of our result in an overall context. ~~An~~[And](#) finally, Section 7 is a summary of our findings.

2 The GROMOS radiometer

The GROund-based Millimeter wave Ozone Spectrometer (GROMOS) is an ozone radiometer, located at the University of Bern (46.95°N, 7.44°E), Switzerland. It is operating continuously since
95 November 1994 in the framework of the Network for the Detection of Atmospheric Composition Change (NDACC).

2.1 Measurement technique

GROMOS is a 142 GHz total power radiometer observing at an elevation angle of 40 degrees in
100 north-east direction. Alternatively, its plane mirror rotates to take measurements from a hot black body (heated to 313 K), the atmosphere (through a microwave transparent styrofoam window) and a cold black body (immersed in liquid nitrogen at 80 K). The hot and cold load measurements are recorded for calibration purposes. The mirror switches position every 8 seconds enabling an accurate black body calibration of the ozone emission line. The detected radiation is led through a quasi optics
105 system, where a Martin-Puplett interferometer (MPI) works as a filter with destructive interference for the radiation at the upper sideband (149.57504 GHz) and constructive interference at 142.17504 GHz. Then the signal is collected by a horn antenna and mixed with the 145.875 GHz wave of a local oscillator for down conversion to an intermediate frequency of 3.7 GHz prior to being analysed by a spectrometer.

110

2.2 Spectrometer upgrade

The spectral analysis was performed by a filter bench (FB) spectrometer from November 1994 to
October 2011. The 45-channel FB had a total bandwidth of 1.2 GHz with individual filters with a
frequency resolution varying from 200 kHz at the line centre to 100 MHz at the wings. Figure 1
115 shows as an example a calibrated spectrum recorded on a winter morning in 2011 by the FB spectrometer, with an integration time of 60 minutes.

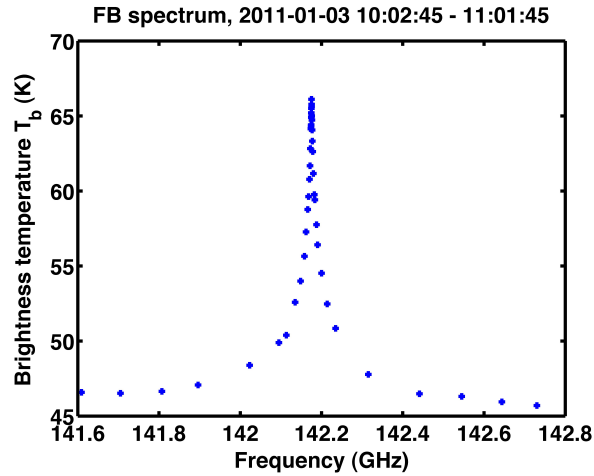


Figure 1. Measurement of the ozone spectrum line at 142 GHz at Bern in a winter day with the filter bench spectrometer. The integration time is 60 minutes.

In July 2009, an Acqiris Fast-Fourier-Transform Spectrometer (FFTS) was added as backend to GROMOS. The FFTS covers a total bandwidth of 1 GHz with 32768 channels, giving a frequency resolution of around 30.5 kHz. A sample of a calibrated ozone spectrum is given in Figure 2. It shows the ozone line recorded by the FFTS on the same winter morning ~~than~~ as the FB spectrum (Figure 1). The integration time is 30 minutes and no frequency binning is applied in the blue curve whereas the red line represents the 15 MHz frequency binned spectrum.

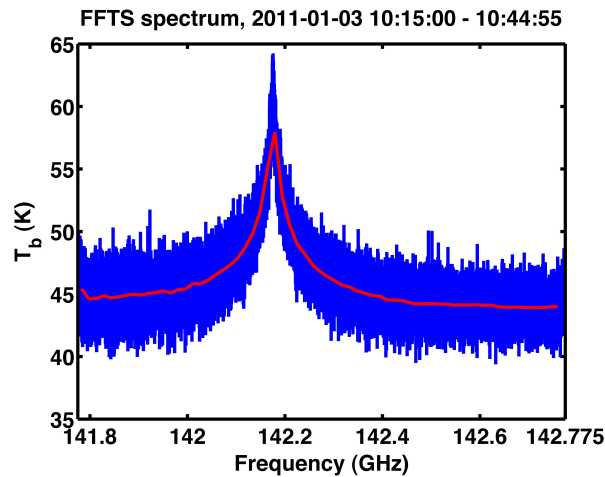


Figure 2. Ozone spectrum line at 142 GHz recorded by the Acqiris FFT Spectrometer at Bern in a winter day. The integration time is 30 minutes. The red line represents the frequency binned.

125 Compared to the FB, the FFTS has a high resolution not only in the centre but also in the line wings. The stability time of our whole radiometer system was improved compared to the FB (Müller

et al., 2009). The FB required much more maintenance by the operator and in spite of this individual channels were disturbed from time to time so that the measured line spectrum was not usable. With the aim to ensure a proper harmonisation of the two datasets, both spectrometers were measuring in parallel for over two years. Afterwards the FB was turned off and FFTS is now used to continue the ozone time series. Table 1 summarises the characteristics of GROMOS radiometer.

Table 1. GROMOS instrument specifications

Location	Bern, Switzerland 46.95°N, 7.44°E, 577 m
Direction of view	North-East
Elevation angle	40°
Mode of operation	Total power
Mixer temperature	294 K (uncooled, room temperature)
System noise temperature	2520 K (single side band)
Frequency of ozone line	142.17504 GHz
Target species	O ₃
Auxiliary quantities	Tropospheric opacity at 142 GHz
Altitude range retrieved	25-70 km
Spectrometer	45-channel FB (Nov.1994-Oct.2011) 32768-channel FFTS (since Jul.2009)
Total bandwidth	1.2 GHz (FB) 1GHz (FFTS)
Frequency resolution	20 kHz at line centre, 100 MHz at line wings (FB) 30.5 kHz (FFTS)
Time resolution for the standard retrieval	60 min (FB) 30 min (FFTS)

2.3 Measurement principle and retrieval procedure

GROMOS measures the thermal microwave emission of a rotational transition of ozone at 142.175 GHz. As the observed emission line is broadened by pressure, the vertical distribution of ozone (approximately from 25 to 70 km) can be calculated from the shape of the observed spectrum in the retrieval procedure. For the ozone profile retrieval of GROMOS, the Atmospheric Radiative Transfer Simulator (ARTS2) (Eriksson *et al.*, 2011) is used as the forward model. It simulates atmospheric radiative transfer and calculates an ozone line spectrum for a model atmosphere using an a priori ozone profile. The accompanying Matlab package Qpack2 (Eriksson *et al.*, 2005) takes advantage of ARTS2 by comparing the modelled spectrum with the observed ozone spectrum of GROMOS. The

Qpack2 derives the best estimate of the vertical profile of ozone volume mixing ratio (VMR) by using the Optimal Estimation Method (OEM) (Rodgers, 1976), and taking into account the uncertainties of the measured ozone spectrum ~~and~~, the a priori profile and the a priori covariance matrix. The OEM further provides a characterisation and formal analysis of the uncertainties (Rodgers, 1990).

145 Prior to the inversion, a tropospheric correction for the tropospheric attenuation (mainly due to water vapour) of stratospheric ozone emission is applied to the calibrated spectra by assuming an isothermal troposphere with a mean temperature, T_{mean} . ~~T_{mean} is the temperature at approximately 2.5 km altitude of the actual temperature profile approaching exponentially the surface value (Peter, 1997).~~ depends upon the temperature profile as well as on the absorption profile at a specific frequency.

150 Since the number density is highest at low altitudes and the absorption is highest near the ground, T_{mean} has a value close to the temperature of the lower troposphere (Ingold *et al.*, 1998). The transmission factor $e^{-\tau} = (T_{B,wing} - T_{mean}) / (T_{B,strat} - T_{mean})$, where τ is the opacity, is estimated from the off-resonance emission $T_{B,wing}$ at the wings of the spectrum and the expected brightness temperature above the troposphere $T_{B,strat}$ (Peter, 1997). The knowledge of the tropospheric opacity

155 permits the so-called tropospheric correction, which means that the effect of tropospheric attenuation is removed from the measured line spectrum (Studer *et al.*, 2014). The inversion is performed for all spectra if the tropospheric opacity is lower than 1.6, i.e. transmission factor larger than 0.2 (Studer *et al.*, 2013). In the standard retrieval, the time resolution is 30 minutes, which gives sufficient signal-to-noise ratio (approximately 30; measurement noise is around 0.7 K and brightness temperature

160 at the ozone line peak is around 20 K) (Studer *et al.*, 2014). The vertical resolution depends upon altitude and can be estimated from the full width at half maximum (FWHM) of a kernel line. The averaging kernels (AVK) and the area of the averaging kernels (AoA) of GROMOS are shown on the middle and right panel of Figure 3. For GROMOS the vertical resolution lies generally within 8-12 km in the stratosphere and increases with altitude to 20-25 km in the lower mesosphere. ~~In the case of GROMOS, the ozone VMR profiles are retrieved with less than 20% of~~ An estimate of the

165 ~~a priori contribution from 30 to 0.3 hPa (altitudes from about 25 to 57 km).~~ to the retrieval can be obtained by the area of the averaging kernels (measurement response). Between 20 to 52 km (50 to 0.5 hPa) the measurement response is higher than 0.8 what corresponds to an a priori contribution less than 20%. Consequently, the retrieved ozone values at these altitudes are predominantly based

170 on the measured line spectrum.

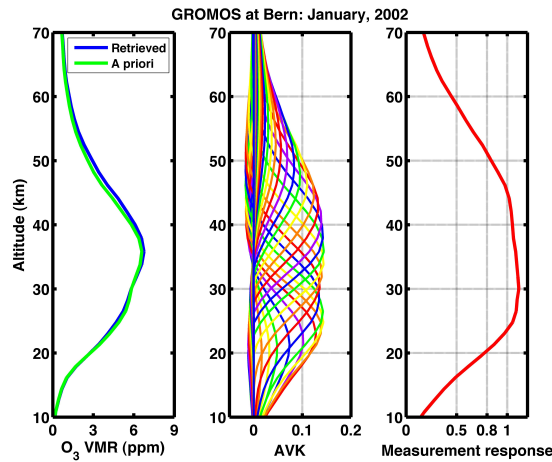


Figure 3. [Example of an a priori profile and a retrieved ozone profile \(left panel\), averaging kernels \(middle panel\) and the measurement response \(area of averaging kernels\) \(right panel\) of the GROMOS retrieval for January, 2002](#)

The a priori profiles of ozone are from a monthly varying climatology based on earlier ozone measurements at Bern. [The As diagonal elements of the a priori covariance matrix we assume a relative error around 35% at 100 hPa. The error decreases in the lower stratosphere up to 28%. Then it increases linearly from 35% in the upper stratosphere to 70% in the lower mesosphere.](#)

175 [The off-diagonal elements exponentially decrease with a correlation length of 3 km. The line shape](#) used in the retrieval is the representation of the Voigt line profile from Kuntz (1997). Spectroscopic parameters to calculate the ozone absorption coefficients were taken from the JPL catalogue (Picket *et al.*, 1998) and the HITRAN spectroscopic database (Rothman *et al.*, 1998). The atmospheric temperature and pressure profiles are taken from the 6 hourly of the European Centre for Medium-
180 Range Weather Forecast (ECMWF) operational analysis data and are extended above 80 km by monthly mean temperatures of the CIRA-86 Atmosphere Model (Fleming *et al.*, 1990). The total error includes systematic error and random error as well as the smoothing term. The systematic error originates from the tropospheric correction, calibration error due to systematic errors in the load temperatures, errors due to baseline features, ~~wrong~~ spectral parameters, etc. The random error
185 includes e.g. the thermal noise on the spectra. An error analysis has been performed by Peter (1997). The uncertainty resulting from the tropospheric correction is smaller than 5% (Ingold *et al.*, 1998). The total error is of the order of 7% for the stratosphere and increases toward the lower and upper altitude limit: up to 10% at 20 km and up to 30% at 70 km. The smoothing term is due to the limited altitude resolution. The GROMOS radiometer is described in more detail by Peter (1997).

190 3 Harmonisation strategy for the ozone profiles

As GROMOS was upgraded with a Fast-Fourier-Transform Spectrometer, an harmonisation is needed between the time series measured by the original Filter Bench (FB) spectrometer and the time series recorded by FFTS. In order to ensure an appropriate harmonisation, both spectrometers were measuring in parallel for over two years. According to subsection **2.2 Spectrometer Upgrade**, the FFTS
195 offers high resolution besides stability and accuracy compared with FB. Therefore, we can use the data recorded by FFTS as reference for the original FB data set.

The strategy carried out for the harmonisation of both data sets was to study the bias between them in the time interval in which both spectrometers were simultaneously measuring, i.e. from October 2009 to August 2011. In Figure 34, we show in the left panel the mean ozone profiles recorded by FB
200 (red line) and by FFTS (blue line), for this time interval. The ~~blue~~ dashed lines are the ~~total error from the retrieval along with the error from the natural variability of FFTS for this time interval. As we are using FFTS data as reference for the FB data and in order to make the figure more straightforward we only show the error profile from FFTS~~ standard deviation of the measurements. The middle panel presents the mean relative difference profile between data of both spectrometers with the FFTS data
205 as reference. The ~~grey dashed lines delimit the FFTS error centred at zero~~ dashed line is the standard deviation of the differences. The bias between FB and FFTS during this overlap period is less than 5% above 20 hPa. The green box indicates the valid range of GROMOS (from 30 to 0.3 hPa). The purpose of the harmonisation is to correct this ~~small~~ bias between both spectrometers, by using the data from FFTS as reference. Accordingly, the harmonisation was performed by subtracting the
210 mean absolute difference profile (right panel) from the FB data set, for every pressure level.

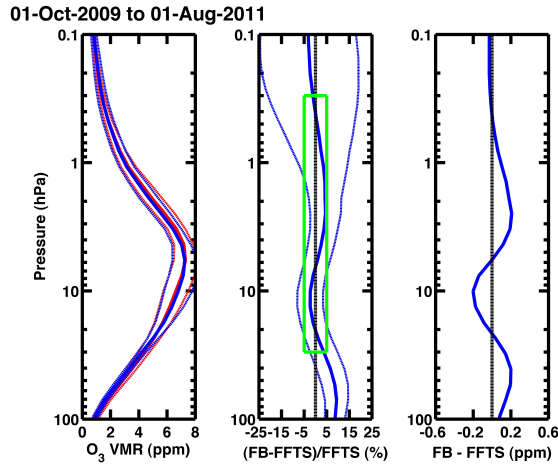


Figure 4. Harmonisation of ozone profiles retrieved from the FB (red line in the left panel) and FFT (blue line in the left panel) spectrometers. The bias between FB and FFTS is less than 5% (middle panel) as derived from the overlap measurement (2009 to 2011) of ozone profiles at pressure levels from 30 to 0.5-0.3 hPa (valid altitude range of GROMOS, green box). The blue dashed lines and the grey dashed lines represent the error of FFTS

On the basis of this harmonisation process, we have generated a time series of 20 years of stratospheric ozone profiles observed by GROMOS over Bern, Figure 45. Undoubtedly, Figure 4-5 provides an extremely clear view of the evolution of stratospheric ozone over the last two decades at a central Europe station, and hence at northern mid-latitudes. Further the annual cycle of ozone can be observed in the stratosphere as well as an increase of mid-stratospheric ozone in last years.

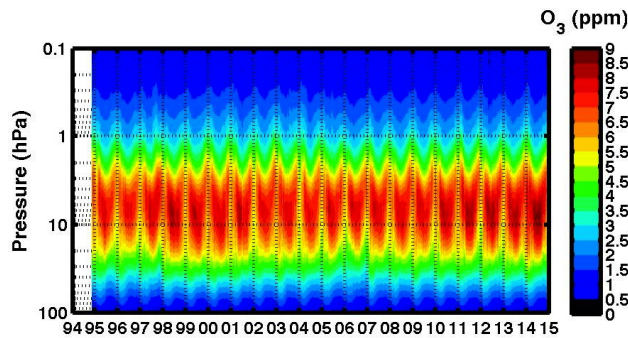


Figure 5. Harmonised 20 years (Nov.1994 - Nov.2014) time series of stratospheric ozone VMR profiles recorded by GROMOS above Bern, Switzerland

4 Trend estimation method

A multilinear parametric trend model (von Clarmann *et al.*, 2010) is applied to the time series of
220 ozone monthly means by fitting the following regression function to the data:

$$\hat{y}(t) = a + b \cdot t + c_1 \cdot qbo_1(t) + d_1 \cdot qbo_2(t) + e \cdot F10.7(t) + f \cdot MEI(t) + \sum_{n=2}^m (c_n \cdot \sin(\frac{2\pi \cdot t}{l_n}) + d_n \cdot \cos(\frac{2\pi \cdot t}{l_n}))$$

(1)

where t is time, a and b represent the constant term and the slope of the fit, respectively. The terms qbo_1 and qbo_2 are the normalised Singapore zonal winds at 30 and 50 hPa as provided by the Free University of Berlin via <http://www.geo.fu-berlin.de/met/ag/strat/produkte/qbo/index.html>.
225 These wind series are approximately orthogonal such that their combination can emulate any Quasi-Biennial Oscillation (QBO) phase shift (Kyrölä *et al.*, 2010). The F10.7 term stands for fitting against the solar 10.7 cm flux, which is commonly used as a measure of solar activity. MEI is the Multivariate ENSO index (MEI), which monitors the El Niño - Southern Oscillation (ENSO) phenomenon with six variables (sea-level pressure, zonal and meridional components of the surface wind, sea sur-
230 face temperature, surface air temperature, and total cloudiness fraction of the sky). Both indices are available from www.esrl.noaa.gov/psd/data/climateindices/list. The sum term comprises 7 sines and cosines functions with the period length l_n , including the annual and semi-annual oscillation as well as 5 harmonics with periods lengths of 3, 4, 7.2, 8.4 and 24 months. The selection of these periods lengths was done by plotting the power spectra of the GROMOS ozone series (Figure 56). In black
235 dotted lines are represented the frequencies for the annual and semi-annual oscillation, the 11 years oscillation due to the solar cycle, the 2.4 years characteristic of the QBO and the 4.5 years frequency related to the ENSO phenomenon. In magenta dotted lines are plotted the spectral components of 24, 8.4, 7.2, 4 and 3 months.

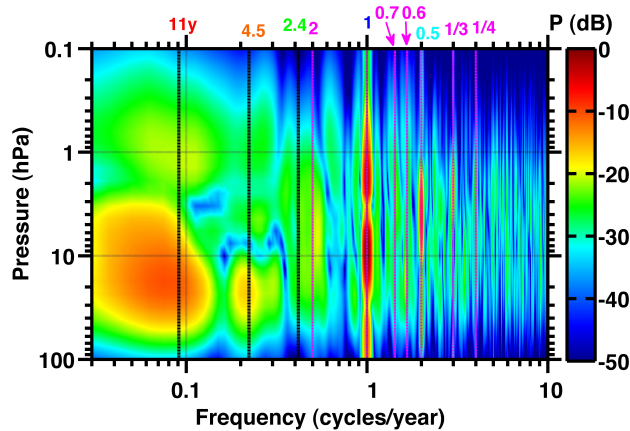


Figure 6. Power spectra of stratospheric ozone time series (Nov.1994 - Nov.2014) measured by GROMOS above Bern, Switzerland. The black dotted lines are the frequencies for the annual and semi-annual oscillation, the 11 years due to the solar cycle, the 2.4 years of the QBO and the 4.5 years of ENSO phenomenon. The magenta dotted lines are the frequencies of the overtones (3, 4, 7.2, 8.4 and 24 months)

With the aim to assess the linear variation of the time series within the period covering November 1994 to November 2014, the coefficients a , b , c_1 , ..., c_8 , d_1 , ..., d_8 , e and f are fitted to the ozone monthly means using the method of von Clarman *et al.* (2010), where the full error covariance matrix of mixing ratios is considered, ~~with the squared standard errors of the monthly means as the diagonal terms (Stiller *et al.*, 2012).~~ The autocorrelations among data points are considered ~~in the covariance matrix, and a model error component is assessed iteratively and added to the covariance matrix in order to account the autocorrelative nature of the atmosphere and to get realistic error estimates.~~ The diagonal elements of the error covariance matrix are the uncertainty of the ozone monthly mean profiles, described in the following section. The off-diagonal elements are initially set zero. In a second iteration, the correlation coefficients between each data-point and its n th neighbour are estimated from the fit residuals, and an additional error term is built, based on these covariances, describing the deficiency of the multi-parametric model chosen. This error term (in terms of covariance matrix) is scaled according to chi-square statistics and added to the initial measurement error covariance matrix.

The inputs required by the trend estimation program are the ozone monthly mean profiles and their uncertainty. An example of the fit is displayed in Figure 67, showing the ozone monthly means as well as the fit and linear variation (top panel) and the residual (middle panel) at 10 hPa. The bottom panel shows the ozone fitted signals of the proxies QBO (blue line), solar F10.7 cm flux (red line) and ENSO (green line), also at 10 hPa. The variability of the GROMOS measurements is satisfactorily reproduced by the fit. The residual is within 0.5 ppmv except for some particular cases.

Most of the ozone variations can be explained by the fitted proxies, maybe due to some short term anomalies.

260

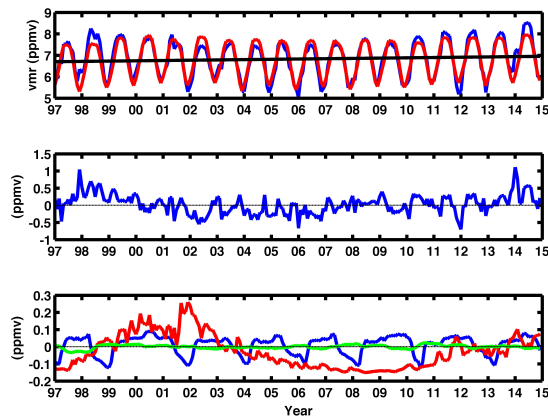


Figure 7. The first panel shows the trend fit at 10 hPa, with the GROMOS monthly mean data (blue line), the calculated fit (red line) and the related trend (black line). The second panel shows the residual and the third panel the fitted signals of the proxies QBO (blue line), solar F10.7 cm flux (red line) and ENSO (green line), at 10 hPa.

5 Uncertainty considerations

Before analysing the estimated trends, the uncertainties affecting the ozone profiles recorded by GROMOS must be considered, analysed and taken into account. We have considered three different ways to assess the types of uncertainties. The first one is the uncertainty of the natural variability that is approximated by the standard error of the monthly mean. The second one is the observation error, which is obtained from the propagation of the thermal noise of the brightness temperature into the ozone profile. The observation error corresponds to the random error, calculated during the retrieval procedure, which is due to the thermal noise on the spectra. The third way to assess the uncertainties is based on cross-validations of GROMOS with satellites and ground-based instruments (Dumitru *et al.*, 2006, Steinbrecht *et al.*, 2006), Studer *et al.*, 2013 and Delcloo and Kreher, 2013).

265

270

The criterion to indicate if an estimated trend is statistically significant at the 95% of confident level is that the absolute ratio of the trend to its uncertainty is larger than 2 (Tiao *et al.*, 1990).

The large number of GROMOS measurements per month allows a robust assessment of the uncertainty from natural variability, where the effect of the autocorrelation among data points within the

275 series is taken into account. The standard error of the monthly mean contains both uncertainties due to measurement noise and atmospheric variability. First the standard deviation has been calculated,

$$\sigma = \frac{1}{n-1} \sum_{i=1}^n (x_i - \bar{x})^2 \quad \sqrt{\frac{1}{n-1} \sum_{i=1}^n (x_i - \bar{x})^2} \quad (2)$$

where n is the number of measurements per month, x the ozone mixing ratio, and \bar{x} its monthly mean. Then the variability within the month has been analysed for autocorrelations between the single measurements. From this information, the degrees of freedom (DGF) have been estimated as
 280 the ratio between the number of measurements n and the correlation length within the month under assessment. Due to the autocorrelations, DGF is less than the number of measurements. For instance if the amount of measurements of GROMOS within a month is around 1300, and at 10hPa the time lag is around 2 days then the DGF are more or less 12.5. Following the same assumption, at 100 hPa
 285 (time lag around 5 days) the DGF are 4.8 and 81.25 at 1hPa (8 hours of time lag). With DGF, the standard error of the monthly mean (SEM) can be calculated:

$$SEM = \frac{\sigma}{\sqrt{DGF}} = \frac{1}{(n-1)\sqrt{DGF}} \sum_{i=1}^n (x_i - \bar{x})^2 \quad \frac{1}{\sqrt{(n-1)DGF}} \sqrt{\sum_{i=1}^n (x_i - \bar{x})^2} \quad (3)$$

To calculate the correlation lengths we have used the autocorrelation function (ACF) of Matlab, which provides us the time lags (correlation lengths) of the temporal autocorrelation function calculations. For stationary processes, the autocorrelation among any two observations only depends on
 290 the time lag. Therefore, the autocorrelation is 1 for the time lag equal to zero, since unlagged data are perfectly correlated with themselves. The collection of autocorrelations, autocorrelation function, computed for various lags exhibit a more or less gradual decay toward zero as the time lag increases, reflecting the generally weaker statistical relationship between data points further remote
 295 from each other in time. The number of time lags of autocorrelated values within the 95% of confidence level are the correlation lengths within a month, used to calculate the DGF.

Finally, ~~owing the fact that we had not taken into account any kind of systematic uncertainty of the instrument, we have chosen to include as uncertainty source an estimation of systematic error profile~~ we assume an uncorrelated monthly instrumental uncertainty. The aim is to take into
 300 account the bias between GROMOS and other instruments, and thereby to get a realistic uncertainty estimation. We have estimated this profile with the result of past-cross validations of coincident data from GROMOS, ozonesondes, nearby lidars and satellites (Dumitru *et al.*, 2006, Steinbrecht *et al.*, 2006), Studer *et al.*, 2013 and Delcloo and Kreher, 2013). Past cross-validations show a systematic
 305 uncertainty of about 5 to 10% for our instrument. Around 5% between 10 and 1 hPa and tending

to roughly 10% toward the lower and upper stratosphere. The strongest point of this estimation method relies on the fact that these validation reports and inter-comparisons cover all the 20 years of GROMOS measurements. Both for the period in which the spectral analysis was done by the filter bench spectrometer (Dumitru *et al.*, 2006, Steinbrecht *et al.*, 2006), as for the period of the new
 310 Fast-Fourier-Transform Spectrometer (Studer *et al.*, 2013, Delcloo and Kreher, 2013).

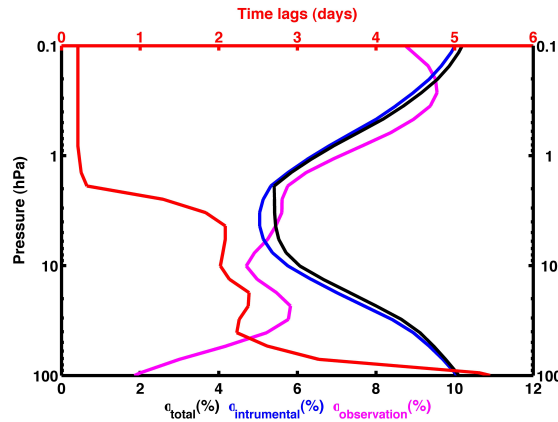


Figure 8. Uncertainty budget of GROMOS used in the trend analysis. The red line is an example of monthly mean correlation length profile, in day units, calculated for the time interval from October 2011 to October 2014. The magenta line is the monthly mean observation error profile, calculated for the same time interval. The ~~black-blue~~ line is the estimated ~~systematic-instrumental~~ error profile. And the ~~blue-black~~ line represents ~~in ppm-VMR~~ the total contribution of the uncertainty of GROMOS.

Figure ~~7-8~~ shows the error budget used as input for the trend estimation model. The red line is an example of monthly mean correlation length profile, in day units, calculated for the time interval from October 2011 to October 2014. We can see the monthly autocorrelations of stratospheric
 315 ozone. The magenta line is the monthly mean observation error profile, from the thermal noise on the spectra, calculated for the same time interval. The ~~black-blue~~ line is the estimated ~~systematic-instrumental~~ error profile based on recent and past intercomparisons of coincident data from GROMOS, ozonesondes, nearby lidars and satellites. And the ~~blue line represents in ppm-VMR~~ ~~black line represents~~ the total contribution of the uncertainty of GROMOS taking into account all the afore-
 320 mentioned errors.

6 Results and discussion

Figure ~~8-9~~ presents the estimated ozone trend profile (in $\% \text{ decade}^{-1}$) for the period of January 1997 - January 2015 above Bern, Switzerland. The selection of the time interval is based on the assumption

325 that 1997 is the turn-around year of the Equivalent Effective Stratospheric Chlorine (EESC), since
 EESC concentration peaked in 1997 at mid-latitudes ([WMO, 2011](#)). The dark blue line represents
 the trend profile, the dark blue area and the light blue area are the 1σ and 2σ areas, respectively.
 Being σ the uncertainty of the trend estimate. The green boxes are the two regions where the trend
 is statistically significant at 95% of confidence level. These features of particular interest are read-
 330 ily identified. The first green box of positive trend between 10 and 2.5 hPa (32 to 42 km) with its
 maximum peak at $(3.14 \pm 1.71)[\% \text{ decade}^{-1}]$ around 4.36 hPa. And the second green box of neg-
 ative trend between 0.6 and 0.06 hPa (50 to 67 km) with its maximum peak at $(-3.94 \pm 2.73)[\% \text{ decade}^{-1}]$
 around 0.2 hPa. The uncertainty denotes twice the standard deviation.

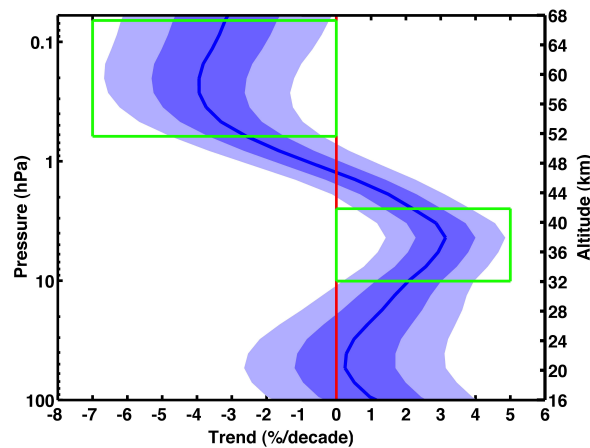


Figure 9. Estimated ozone trend profile (in $\% \text{ decade}^{-1}$) for the period of January 1997 - January 2015 recorded by GROMOS above Bern, Switzerland. The dark blue line represents the trend profile, the darkest blue area and the lightest blue area are the 1σ and 2σ areas, respectively. Being σ the uncertainty of the trend estimate. The green boxes are the two regions where the trend is statistically significant at 95% of confidence level.

335 The estimated stratospheric trend results are able to support the evidence of shift toward increas-
 ing ozone in the middle and upper stratosphere at northern mid-latitudes also reported by previ-
 ous studies (Vigouroux *et al.*, 2008; Nair *et al.*, 2013; Huang *et al.*, 2014; WMO, 2014; Tummon
et al., 2015; and references therein). On the other hand, other recent studies ([Eckert *et al.*, 2014](#) ;
[Vigouroux *et al.*, 2015](#) ; [Harris *et al.*, 2015](#) ; and references therein) have found positive but not sig-
 340 nificant trend in our location. But we have to be careful about these discrepancies since it could arise
 from differences in treatment and propagations of uncertainties, selection of data, ozone measure-
 ment techniques, statistical approach, latitudinal and altitudinal extent and/or the time period covered
 in the trend study([Eckert *et al.*, 2014](#) ; [Vigouroux *et al.*, 2015](#) ; [Harris *et al.*, 2015](#) ; and references
 therein).

345 The WMO (2014, [Table 2.4](#)) reported a statistically significant ozone increase of [2.5-5% per decade](#) ([3.9](#)

± 1.3 (% decade⁻¹) at 40 km in the upper stratosphere at northern mid-latitudes (35-60 °N) over the 2000-2013 period. The stated range encompasses the mean values with ± 2 standard error range. This ozone trend value is based on observations from various space-based and ground-based measurement instruments. A slightly different ozone series of the GROMOS instrument contributed a bit to the ozone trend estimation of WMO (2014). The ozone trend of our study cannot be directly compared to WMO (2014) since the time window and the measurement region differ. However, the ozone trend at Bern (about 3.0%/decade at 40 km) agrees well with the ozone trend at northern mid-latitudes (about 3.9%/decade at 40 km) as reported by WMO (2014). Furthermore, Nair *et al.* (2013) presented positive upper stratospheric ozone trends, in the 1997-2010 period, over a northern mid-latitude station, Haute-Provence Observatory (OHP: 43.93°N, 5.71°E), using GOZCARDS (Global Ozone Chemistry And Related trace gas Data records for the Stratosphere) data and a combination of data sets from total column ozone observations from the Dobson and Système d'Analyse par Observation Zénithale (SAOZ) spectrometers and ozone profile measurements from the light detection and ranging (lidar), ozonesondes, Stratospheric Aerosol and Gas Experiment (SAGE) II, Halogen Occultation Experiment (HALOE) and Aura Microwave Limb Sounder (MLS). Our results also match well with those reported in WMO (2010) and by Vigouroux *et al.* (2008), who deduced a positive trend of (0.26 ± 0.18) [% year⁻¹] at Jungfraujoch for the period 1995-2004 in the altitude range between 27-42 km. The Jungfraujoch station located in Switzerland at 47°N is equipped with a Fourier Transform infrared (FTIR) instrument. Moreover, Tummon *et al.* (2015) showed, with Solar Backscatter Ultraviolet Radiometer (SBUV) instruments on-board NASA (National Aeronautics and Space Administration) and NOAA (National Oceanographic and Atmospheric Administration) satellites, significant positive trends up to 4 % decade⁻¹ between 10-7 hPa, for the 1998-2011 period. All these statements are in agreement with our findings. The small change in trends is somewhat to be expected given that the lifetimes of most ozone depleting substances (ODS) species are long (several decades) and thus the removal of these species will occur over a considerably longer timescale than the relatively brief period during which their concentrations increased (Tummon *et al.*, 2015). Otherwise, the increase of carbon dioxide is cooling the upper stratosphere. This cooling increases ozone concentrations in this region through temperature-dependent chemistry (WMO, 2014).

Concerning circulation changes as contributors to the stratospheric ozone increases, recent studies have simulated changes in the Brewer-Dobson circulation (BDC) in response to increasing greenhouse gases (Butchart *et al.*, 2006). Changes in the BDC can modify the distribution of ozone and other chemical compounds. Recently this stratospheric mean meridional circulation (BDC) has been clearly differentiated into two branches: a shallow branch, located in the lowermost stratosphere, with upwelling in the tropics and downwelling in the subtropics and middle latitudes, and a deep branch with maximum upwelling in the tropical upper stratosphere and downwelling in the middle and high latitudes throughout the entire height of the stratosphere (Birner and Bönisch, 2011). Observations of changes in temperature and ozone over the past three to five decades are sugges-

tive of increased upwelling of air in the tropical lower stratosphere. This is consistent with model simulations, which robustly simulate long-term increases in the tropical upwelling due to past greenhouse gas increases (WMO, 2014). Ozone in the tropical lower stratosphere shows little response to ODS, because conversion of ODS into reactive chlorine and bromine is small in this region. Instead, tropical lower stratospheric ozone is more affected by the strength of tropical upwelling of air from troposphere to stratosphere caused by the shallow branch of the BDC (WMO, 2014). Additionally, Stiller *et al.* (2012) also used the hypothesis of a general increased upwelling in the tropics and intensification of the BDC, together with weakening of the subtropical mixing barrier as an explanation of their age of air temporal evolution. Therefore, the acceleration of both branches of BDC could be one of the contributors to the aforementioned stratospheric ozone increase in northern mid-latitudes. Regarding the lower mesosphere region, our results are in agreement with recent trend estimations (Kyrölä *et al.*, 2013; Remsberg, 2014 and references therein; Tummon *et al.*, 2015). They have found statistically significant negative trends above 55 km in the northern mid-latitudes through the SAGE II (Stratospheric Aerosol and Gas Experiment) version 7 data and by the combined SAGE II-GOMOS (Global Ozone Monitoring by Occultation of Stars) data set.

7 Conclusions

We have constructed an harmonised ozone profile time series from GROMOS measurements since November 1994 up to now. The need for such harmonisation is due to the spectrometer upgrade performed in 2009. From November 1994 to October 2011, the ozone line spectra were measured by a filter bench spectrometer (FB). Since July 2009 the spectral analysis is done by a Fast-Fourier-Transform Spectrometer (FFTS). Both spectrometers were measuring parallel in order to ensure a proper harmonisation. A bias between both data sets has been identified, being less than 5% above 20 hPa. The harmonisation has been done by taking the data set from the FFTS as reference for the FB. The combined data set time series was then analysed for trends in the stratosphere.

A multilinear parametric trend model was used to analyse this 20 years of stratospheric ozone profiles. This model includes a linear term, the solar variability, the El Niño - Southern Oscillation (ENSO) index, the quasi-biennial oscillation (QBO), the annual and semi-annual oscillation and several harmonics with period lengths between 3 and 24 months. The trend results for the period between January 1997 and January 2015 show statistically significant trends at 95% level at pressure levels around 5 and 0.2 hPa. Our estimated trend profile is in agreement with other northern mid-latitude trend estimations from other ground-based and satellite instruments (Vigouroux *et al.*, 2008; Nair *et al.*, 2013; Kyrölä *et al.*, 2013; Huang *et al.*, 2014; Remsberg, 2014 ; WMO, 2014; Tummon *et al.*, 2015, and references therein).

This study also demonstrates the reliability of GROMOS measurements for providing stratospheric ozone profiles. Allowing us the adequate study of the characterisation of ozone variability on time

scales from 10 minutes to more than 20 years. The continuation in time with these measurements will help future generations to confirm findings through the intercomparison with other instruments and to understand the evolution of the ozone layer that is extremely crucial for life on Earth.

420

Acknowledgements. This work was supported by the Swiss National Science Foundation under Grant 200020 - 160048 and MeteoSwiss GAW Project: "Fundamental GAW parameters measured by microwave radiometry".

References

- Birner, T. and Bönisch, H.: Residual circulation trajectories and transit times into the extratropical lowermost stratosphere, 2, 817-827, doi:10.5194/acp-11-817-2011, 2011
- 425 Butchart, N., Scaife, A. A., Bourqui, M., de Grandpré, J., Hare, S. H. E., Kettleborough, J., Langematz, U., Manzini, E., Sassi, F., Shibata, K., Shindell, D. and Sigmond, M.: Simulations of anthropogenic change in the strength of the Brewer-Dobson circulation, 27, 727-741, doi:10.1007/s00382-006-0162-4, 2006
- Delcloo, A., and Kreher, K.: O3M SAF Validation report, Finish Meteorological Institute, available at: http://o3msaf.fmi.fi/docs/vr/Validation_Report_NOP_NHP_OOP_OHP_Jun_2013.pdf (last access: 16 June 2015), 2013.
- 430 Dumitru, M. C., Hocke, K., Kämpfer, N., and Calisesi, Y.: Comparison and validation studies related to ground-based microwave observations of ozone in the stratosphere and mesosphere, *J. Atmos. Sol.-Terr. Phys.*, 68, 745-756, 2006
- 435 Eckert, E., von Clarmann, T., Kiefer, M., Stiller, G. P., Lossow, S., Glatthor, N., Degenstein, D. A., Froidevaux, L., Godin-Beekmann, S., Leblanc, T., McDermid, S., Pastel, M., Steinbrecht, W., Swart, D. P. J., Walker, K. A., and Bernath, P. F.: Drift-corrected trends and periodic variations in MIPAS IMK/IAA ozone measurements, *Atmos. Chem. Phys.*, 14, 2571-2589, doi:10.5194/acp-14-2571-2014, 2014
- Eriksson, P., Jiménez, C., and Buehler, S. A.: Qpack, a general tool for instrument simulation and retrieval work, 440 *J. Quant. Spectrosc. Ra.*, 91, 47-64, doi:10.1016/j.jqsrt.2004.05.050, 2005
- Eriksson, P., Buehler, S. A., Davis, C. P., Emde, C., and Lemke, O.: ARTS, the atmospheric radiative transfer simulator, Version 2, *J. Quant. Spectrosc. Ra.*, 112, 1551-1558, doi:10.1016/j.jqsrt.2011.03.001, 2011
- Fleming, E.L., Chandra S., Barnett J.J. and Corney, M.: Zonal mean temperature, pressure, zonal wind, and geopotential height as functions of latitude, COSPAR International Reference Atmosphere: 1986, Part II: 445 Middle Atmosphere Models, *Adv. Space Res.*, 10, 12, 11-59, doi:10.1016/0273-1177(90)90386-E, 1990
- Harris, N. R. P., Hassler, B., Tummon, F., Bodeker, G. E., Hubert, D., Petropavlovskikh, I., Steinbrecht, W., Anderson, J., Bhartia, P. K., Boone, C. D., Bourassa, A., Davis, S. M., Degenstein, D., Delcloo, A., Frith, S. M., Froidevaux, L., Godin-Beekmann, S., Jones, N., Kurylo, M. J., Kyrölä, E., Laine, M., Leblanc, S. T., Lambert, J. C., Liley, B., Mahieu, E., Maycock, A., de Mazière, M., Parrish, A., Querel, R., Rosenlof, K., 450 H., Roth, C., Sioris, C., Staehelin, J., Stolarski, R. S., Stübi, R., Tamminen, J., Vigouroux, C., Walker, K., Wang, H. J., Wild, J. and Zawodny, J. M.: Past changes in the vertical distribution of ozone - Part 3: Analysis and interpretation of trends, *Atmos. Chem. Phys. Discuss.*, 15, 8565-8608, doi:10.5194/acpd-15-8565-2015, 2015
- Huang, F. T., Mayr, H. G., Russell III, J. M., and Mlyneczek, M. G.: Ozone and temperature decadal trends in the stratosphere, mesosphere and lower thermosphere, based on measurements from SABER and TIMED, 455 *Ann. Geophys.*, 32, 935-949, doi:10.5194/angeo-32-935-2014, 2014
- Hudson, R. D. and Reed, E. I.: The stratosphere: Present and future, NASA Ref. Pub. 1049, Washington, D. C., 432pp., 1979
- Ingold, T., Peter, R., and Kämpfer, N.: Weighted mean tropospheric temperature and transmittance determination at millimeter-wave frequencies for ground-based application, *Radio Sci.*, 33, 905-918, 1998
- 460 [Keckhut, P., Hauchecorne, A., Blanot, L., Hocke, K., Godin-Beekmann, S., Bertaux, J.-L., Barrot, G., Kyrölä, E., van Gijsel, J. A. E., and Pazmino, A.: Mid-latitude ozone monitoring with the](#)

- [GOMOS-ENVISAT experiment version 5: the noise issue, Atmos. Chem. Phys., 10, 11839-11849, doi:10.5194/acp-10-11839-2010, 2010.](#)
- 465 Kyrölä, E., Laine, M., Sofieva, V., Tamminen, J., Päivärinta, S.-M., Tukiainen, S., Zawodny, J., and Thomason, L.: Combined SAGE-GOMOS ozone profile data set for 1984-2011 and trend analysis of the vertical distribution of ozone, *Atmos. Chem. Phys.*, 13, 10645-10658, doi:10.5194/acp-13-10645-2013
- Kyrölä, E., Tamminen, J., Sofieva, V., Bertaux, J. L., Hauchecorne, A., Dalaudier, F., Fussen, D., Vanhellemont, F., Fanton d'Andon, O., Barrot, G., Guirlet, M., Fehr, T., and Saavedra de Miguel, L.; GOMOS O₃, NO₂, and NO₃ observations in 2002-2008, *Atmos. Chem. Phys.*, 10, 7723-7738, doi:10.5194/acp-10-7723-2010, 2010
- Kuntz, M.: A new implementation of the Humlicek algorithm for the calculation of the Voigt profile function, *J. Quant. Spectrosc. Ra.*, 57, 819-824, doi:10.1016/S0022-4073(96)00162-8, 1997
- Molina, M. J. and Rowland, F. S.: Stratospheric sink for chlorofluoromethanes: Chlorine atom catalyzed destruction of ozone, *Nature*, 249, 810-812, doi:10.1038/249810a0, 1974
- 475 Müller, S., Murk A., Monstein, C., and Kämpfer, N.: Intercomparison of digital Fast Fourier Transform and Acoustooptical Spectrometers for microwave radiometry of the atmosphere, *IEEE T. Geosci. Remote*, 47, 2233-2239, doi:10.1109/TGRS.2009.2013695, 2009
- Nair, P. J., Godin-Beekmann, S., Kuttippurath, J., Ancellet, G., Goutail, F., Pazmiño, A., Froidevaux, L., Zawodny, J. M., Evans, R. D., Wang, H. J., Anderson, J., and Pastel, M.: Ozone trends derived from total columns and vertical profiles at a northern mid-latitude station, *Atmos. Chem. Phys.*, 13, 10373-10384, doi:10.5194/acp-13-10373-2013, 2013
- 480 [Newchurch, M. J., E.-S. Yang, D. M. Cunnold, G. C. Reinsel, J. M. Zawodny, and J. M. Russell III, Evidence for slowdown in stratospheric ozone loss: First stage of ozone recovery, J. Geophys. Res., 108, 4507, doi:10.1029/2003JD003471, 2003](#)
- 485 Palm, M., Hoffmann, C. G., Golchert, S. H. W., and Notholt, J.: The ground-based MW radiometer OZORAM on Spitsbergen - description and status of stratospheric and mesospheric O₃-measurements, *Atmos. Meas. Tech.*, 3, 1533-1545, doi:10.5194/amt-3-1533-2010, 2010
- [Parrish, A., B. J. Connor, J. J. Tsou, I. S. McDermid, and W. P. Chu, Ground-based microwave monitoring of stratospheric ozone, J. Geophys. Res., 97\(D2\), 2541-2546, doi:10.1029/91JD02914, 1992](#)
- 490 Peter R.: The ground-based millimeter-wave ozone spectrometer-GROMOS, IAP Research Report, University of Bern, Bern, Switzerland, 13, 1997
- Pickett, H. M., Poynter, R. L., Cohen, E. A., Delitsky, M. L., Pearson, J. C., and Müller, H. S. P.: Submillimeter, millimeter, and microwave spectral line catalog, *J. Quant. Spectrosc. Ra.*, 60, 883-890, doi:10.1016/S0022-4073(98)00091-0, 1998
- 495 Remsberg, E. E.: Decadal-scale responses in middle and upper stratospheric ozone from SAGE II version 7 data, *Atmos. Chem. Phys.*, 14, 1039-1053, doi:10.5194/acp-14-1039-2014
- Rodgers, C. D.: Retrieval of atmospheric temperature and composition from remote measurements of thermal radiation, *Rev. Geophys. Space Ge.*, 14, 609-624, 1976
- 500 Rodgers, C. D.: Characterisation and error analysis of profiles retrieved from remote sounding measurements, *J. Geophys. Res.-Atmos.*, 95, 5587-5595, doi:10.1029/JD095iD05p05587, 1990

- Rothman, L., Rinsland, C., Goldman, A., Massie, S. T., and Edwards, D. P.: The HITRAN molecular spectroscopic database and HAWKS (HITRAN atmospheric workstation): 1996 edition, *J. Quant. Spectrosc. Ra.*, 60, 665-710, doi:10.1016/S0022-4073(98)00078-8, 1998
- 505 Steinbrecht, W., Claude, H., Schöenborn, F., McDermid, I., Leblanc, T., Godin, S., Song, T., Swart, D., Meijer, Y., Bodeker, G., Connor, B., Kämpfer, N., Hocke, H., Calisesi, Y., Schneider, N., Noe, J., Parrish, A., Boyd, I., Brühl, C., Steil, B., Giorgetta, M., Manzini, E., Thomasson, L., Zawodny, J., McCormick, M., Russel III, J., Bhartia, P., Stolarski, R., and Hollandsworth-Frith, S.: Long-term evolution of upper stratospheric ozone at selected stations of the Network for the Detection of Stratospheric Change (NDSC), *J. Geophys. Res.*, 510 111, D10308, doi:10.1029/2005JD006454, 2006
- [Steinbrecht, W., McGee, T. J., Twigg, L. W., Claude, H., Schöenborn, F., Sumnicht, G. K., and Silbert, D.: Intercomparison of stratospheric ozone and temperature profiles during the October 2005 Hohenpeissenberg Ozone Profiling Experiment \(HOPE\), *Atmos. Meas. Tech.*, 2, 125-145, doi:10.5194/amt-2-125-2009, 2009.](#)
- 515 Stillner, G. P., von Clarmann, T., Haenel, F., Funke, B., Glatthor, N., Grabowski, U., Kellmann, S., Kiefer, M., Linden, A., Lossow, S., and López-Puertas, M.: Observed temporal evolution of global mean age of stratospheric air for the 2002 to 2010 period, *Atmos. Chem. Phys.*, 12, 3311-3331, doi:10.5194/acp-12-3311-2012, 2012
- Studer, S. and Hocke, Schanz, A., Schmidt, H., and Kämpfer, N.: A climatology of the diurnal variations in stratospheric and mesospheric ozone over Bern, Switzerland *Atmos. Chem. Phys.*, 14, 5905-5919, 520 doi:10.5194/acp-14-5905-2014
- Studer, S. and Hocke, K., Pastel, M., Godin-Beekmann, S. and Kämpfer, N.: Intercomparison of stratospheric ozone profiles for the assessment of the upgraded GROMOS radiometer at Bern, *Atmos. Meas. Tech. Discuss.*, 6, 6097-6146, doi:10.5194/amtd-6-6097-2013, 2013
- 525 Tiao, G. C., Reinsel, G. C., Xu, D., Pedrick, J. H., Zhu, X., Miller, A. J., DeLuisi, J. J., Mateer, C. L., and Wuebbles, D. J.: Effects of autocorrelation and ~~tempotal~~temporal sampling schemes on estimates of trend and spatial correlation, *J. Geophys. Res.*, 95, 20507-20517, doi:10.1029/JD095iD12p20507, 1990
- Tummon, F., Hassler, B., Harris, N. R. P., Staehelin, J., Steinbrecht, W., Anderson, J., Bodeker, G. E., Bourassa, A., Davis, S. M., Degenstein, D., Frith, S. M., Froidevaux, L., Kyrölä, E., Laine, M., Long, C., Penckwitt, A. A., Sioris, C. E., Rosenlof, K. H., Roth, C., Wang, H. J. and Wild, J.: Intercomparison of vertically resolved 530 merged satellite ozone data sets: interannual variability and long-term trends, *Atmos. Chem. Phys.*, 15, 3021-3043, doi:10.5194/acp-15-3021-2015, 2015
- [van Gijsel, J. A. E., Swart, D. P. J., Baray, J.-L., Bencherif, H., Claude, H., Fehr, T., Godin-Beekmann, S., Hansen, G. H., Keckhut, P., Leblanc, T., Mc-Dermid, I. S., Meijer, Y. J., Nakane, H., Quel, E. J., Stebel, K., Steinbrecht, W., Strawbridge, K. B., Tatarov, B. I., and Wolfram, E. A.: GOMOS ozone profile validation using ground-based and balloon sonde measurements, *Atmos. Chem. Phys.*, 10, 473-488, doi:10.5194/acp-10-473-2010, 2010](#)
- 535 Vigouroux, C., Blumenstock, T., Coffey, M., Errera, Q., García, O., Jones, N. B., Hannigan, J. W., Hase, F., Liley, B., Mahieu, E., Mellqvist, J., Notholt, J., Palm, M., Persson, G., Schneider, M., Servais, C., Smale, D., Thölix, L. and De Mazière, M.: Trends of ozone total columns and vertical distribution from FTIR observations at eight NDACC stations around the globe, *Atmos. Chem. Phys.*, 15, 2915-2933, doi:10.5194/acp-15-2915-2015, 2015

- Vigouroux, C., De Mazière, M., Demoulin, P., Servais, C., Hase, F., Blumenstock, T., Kramer, I., Schneider, M., Mellqvist, J., Strandberg, A., Velazco, V., Notholt, J., Sussmann, R., Stremme, W., Rockmann, A., Gardiner, T., Coleman, M. and Woods, P.: Evaluation of tropospheric and stratospheric ozone trends over Western Europe from ground-based FTIR network observations, *Atmos. Chem. Phys.*, 8, 6865-6886, doi:10.5194/acp-8-6865-2008, 2008
- 545
- von Clarmann, T., Stiller, G., Grabowski, U., Eckert, E., and Orphal, J.: Technical note: Trend estimation from irregularly sampled correlated data, *Atmos. Chem. Phys.*, 10, 6737-6747, doi:10.5194/acp-10-6737-2010, 2010
- 550
- WMO (World Meteorological Organisation), *Scientific Assessment of Ozone Depletion: 2010*, Global Ozone Research and Monitoring Project-Report No. 52, 516 pp., Geneva, Switzerland, 2011
- WMO (World Meteorological Organisation), *Scientific Assessment of Ozone Depletion: 2014*, Global Ozone Research and Monitoring Project - Report No. 55, 416 pp., Geneva, Switzerland, 2014